The Head-Body-Tail Intersection for Spatial Relations Between Directed Line Segments

Yohei Kurata and Max J. Egenhofer

National Center for Geographic Information and Analysis
and
Department of Spatial Information Science and Engineering
University of Maine
Boardman Hall, Orono, ME 04469-5711, USA
{yohei, max}@spatial.maine.edu

Abstract. Directed line segments are fundamental geometric elements used to model through their spatial relations such concepts as divergence, confluence, and interference. A new model is developed that captures spatial relations between pairs of directed line segments through the intersections of the segments' heads, bodies, and tails. This *head-body-tail intersection* identifies 68 classes of topological relations between two directed line segments highlighting two equal-sized subsets of corresponding relations that differ only by their empty and non-empty body-body intersections. The relations' conceptual neighborhood graph takes the shape of a torus inside a torus, one for each subset. Another 12 classes of topological relation classes are distinguished if the segments' exteriors are considered as well, lining up such that their conceptual neighborhood graph forms another torus that contains the other two tori. These conceptual neighborhoods as well as the relations' composition table enable spatial inferences and similarity assessments in a consistent and reasoned manner.

1 Introduction

Directed line segments (called *DL segments*) are fundamental geometric elements used in geographic databases to represent directed linear entities, such as one-way roads and watercourses. People also often employ arrow symbols, an expressive form of DL segments, to display dynamic phenomena, for instance, movement, interaction, causality, and change (Kurata and Egenhofer 2005b), and their spatial relations illustrate such scenarios as divergence, confluence, and interference (Kurata and Egenhofer 2006). Geographic databases have a tradition of processing spatial queries over line segments (Hoel and Samet 1991) and spatio-temporal database systems have been increasingly adding corresponding relations into query languages to enable the retrieval and analysis of spatio-temporal configurations at a high level of abstraction (Erwig and Schneider 1999). To further advance spatial query languages for directed linear element, and to supply a basis for the interpretation of the semantics of route

graphs (Krieg-Brückner and Shi, 2005) to communicate route descriptions in a meaningful way, formal models of spatial relations between DL segments and comprehensive reasoning mechanisms about those relations are needed. In comparison to the well-established methods for topological relations for regions, however, models of relations among DL segments have attracted only little attention. Since DL segments are 1-dimensional objects embedded in a 2-dimensional space, they have more degrees of freedom than regions in the same space, which is a property of DL segments that makes reasoning with them more intricate. This paper's scope is on those spatial relations that are invariant under topological transformations of the embedding space. Metric properties can be used subsequently to provide refinements of the resulting relations in analogy to the way line-line relations have been enhanced metrically (Nedas *et al.* in press).

Throughout the rest of this paper DL segments are illustrated as arrow symbols, which are essentially DL segments that are constrained such that they typically refer to (i.e., originate from, traverse, and point to) other elements in a diagram, thereby establishing the semantics of these related elements (Kurata and Egenhofer 2005a), whereas generic DL segments are often used independently. We focus on the direct relations between DL segments, which are formed by their mutual intersections, and do not consider indirect relations, which are materialized by other elements. Each DL segment is further assumed to be embedded in a 2-dimensional space and not to intersect with itself.

The remainder of this paper is structured as follows: Section 2 reviews models for line-line relations. Section 3 classifies the topological relations between two DL segments based on the intersections between the lines' heads, bodies, and tails (called the hbt-intersection), yielding 68 classes of DL relations. Section 4 schematizes these 68 classes by their conceptual neighborhood graph, thereby arranging the relations according to their similarities. Section 5 develops the relations' composition table, forming a formal foundation for qualitative reasoning about DL segments. Section 6 analyzes the effect of considering—in addition to the DL segments' heads, bodies, and tails—also their exteriors, rendering a DL relation model that identifies another twelve classes. Section 7 concludes with a discussion of future work items.

2 Models of Line-Line Relations

Binary relations between line segments in $\mathbb{R}^2$ (and their lower-dimensional relatives, temporal intervals in $\mathbb{R}^1$) have been studied extensively in artificial intelligence and spatio-temporal databases. Allen (1983) identified thirteen order relations between two temporal intervals embedded in $\mathbb{R}^1$. The *4-intersection* (Egenhofer and Franzosa 1991) captures the topological relations between two objects based on the existence/non-existence of geometric intersections between the objects' interiors and boundaries. For non-directed line segments in $\mathbb{R}^1$, it identifies eight topological relations (Pullar and Egenhofer 1988), essentially the same as for two regions in $\mathbb{R}^2$,

and distinguishes sixteen binary relations between two lines in $\mathbb{R}^2$, without capturing an equivalence relation (Hadzilacos and Tryfona 1992). The dimension-extended method of the 4-intersection (Clementini *et al.* 1993) finds eighteen line-line relations. The *9-intersection* (Egenhofer and Herring 1991) extends the 4-intersection by considering also the intersections with respect to the objects' exteriors, which gives rise to distinguishing formally 33 topological relations between two non-directed line segments in $\mathbb{R}^2$ (Egenhofer 1994). Another variation of the 4-intersection distinguishes explicitly the two boundaries (i.e., endpoints) of a line segment, identifying sixteen relations between two intervals in a temporal cycle, which are equivalent to topological relations between uni-directed line segments embedded in a cyclic 1-dimensional space (Hornsby *et al.* 1999). Models for detailed topological relations, capturing for non-empty intersections such properties as sequences of crossing types, intersection dimensions, and orientations of common segments, have been developed for region-region relations (Egenhofer and Franzosa 1995) and line-line relations (Clementini and di Felice, 1998), yielding a set of *topological invariants*. Such additional invariants of component intersections have been known to be germane to distinguishing even basic line-line relations, such as touching from crossing (Herring 1991). Nedas *et al.* (in press) provided metric refinements for detailed topological relations between line segments by incorporating two metric measures, *splitting ratios* and *closeness measures*, into the 9-intersection matrix and the topological invariants.

Conceptual neighborhood graphs, which establish links among relations to capture similarities among them, have been developed for a series of spatial and temporal relations (Egenhofer and Al-Taha 1992, Freska 1992a, Egenhofer and Mark 1995, Papadias *et al.* 1995, Schlieder 1995, Hornsby *et al.* 1999, Egenhofer 2005) to support qualitative analyses of change and to provide the foundations for computational similarity models over spatial relations (Egenhofer 1997) as well as a rationale for modeling the semantics of natural-language spatial predicates (Mark and Egenhofer 1994, Shariff *et al.* 1998). Several increments towards the identification of a conceptual neighborhood graph of line-line relations have been made, starting with Freksa's (1992a) neighborhood graphs of Allen's thirteen interval relations. A fragment of a conceptual neighborhood graph for line-line relations in $\mathbb{R}^2$ (Egenhofer *et al.* 1993) was recently incremented (Reis *et al.* 2005), but lacks the comprehensive treatment found for other relations. Apparently the degree of freedom for lines in a higher-dimensional space leads to an increased complexity for identifying those pairs of relations for which atomic transformations in the spirit of the conceptual neighborhood similarity are feasible.

In addition to topological relations, spatial relations of line segments have been categorized based on order and direction. The *double-cross* (Freksa 1992b) introduces left/right and front/back dichotomies to capture qualitative directions, yielding 15 direction relations from an observer's point to a target. Another approach, based on Allen's interval relations, identifies 63 order relations (essentially directional relations) between two straight DL segments in $\mathbb{R}^2$ (Schlieder 1995). The *dipole calculus* (Moratz *et al.* 2000) is based on 24 directional relations between two straight DL segments in $\mathbb{R}^2$, which fulfill the constraints of a relation algebra. Likewise, 26

order relations between two directed intervals in $\mathbb{R}^1$ form the *directed interval algebra* (Rentz 2001). The *Direction-Relation Matrix* provides an overall framework for describing direction relations between any pair of extended objects in $\mathbb{R}^2$, including arbitrarily shaped lines (Goyal and Egenhofer 2000).

3   Classes of Topological Relation Between DL Segments

A *DL segment* consists of two distinct points, a non-self-intersecting, continuous line that connects the two points, and an orientation imposed on the line, which categorizes the two points as start and end points. Following principles from algebraic topology (Alexandroff 1961), the two points form the *boundary* of a DL segment, whereas the connection between the points forms the *interior*. Due to the geometric similarity of DL segments and arrow symbols, the binary topological relations between DL segments are captured like the topological relations between two arrow symbols (Kurata and Egenhofer 2006), that is, based on the intersections between their interiors (the *body* X°) and the two ordered boundaries (*head* $\partial_{head}X$ and *tail* $\partial_{tail}X$). These nine intersections yield the DL segments' *head-body-tail-intersection* (*hbt-intersection*), which is concisely represented by a 3×3 matrix, called the *hbt-matrix* for DL segment relations (Eqn. 1).

$$M_I(A,B) = \begin{pmatrix} \partial_{tail}A \cap \partial_{tail}B & \partial_{tail}A^\circ \cap B^\circ & \partial_{tail}A \cap \partial_{head}B \\ A^\circ \cap \partial_{tail}B & A^\circ \cap B^\circ & A^\circ \cap \partial_{head}B \\ \partial_{head}A \cap \partial_{tail}B & \partial_{head}A \cap B^\circ & \partial_{head}A \cap \partial_{head}B \end{pmatrix} \qquad (1)$$

Like for line-line relations, each intersection could be analyzed for various topological invariants, such as its dimension, the number of intersections, and the type of intersection, but we choose the most fundamental property, that is, whether each intersection is empty (ϕ) or non-empty ($\neg\phi$). The empty/non-empty entries of the hbt-matrix are constrained among each other since the first and third column, as well as the first and third row, have at most one non-empty entry, because the head or tail of a DL segment is a point, which cannot intersect with more than one part of another DL segment. Among the $2^9 = 512$ configurations of a 3×3 matrix with empty or non-empty entries, only 68 cases satisfy this constraint (Tables 1 and 2). Each of these 68 configurations corresponds to a different set of topological relations (Fig. 1), while the remaining 444 configurations have no valid geometric interpretations. In this way,
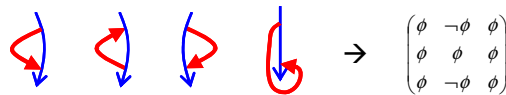
Fig. 1. Five different topological relations between two DL segments with the same hbt-matrix, which implies that the hbt-intersection groups this set of DL relations into the same TR-class

the hbt-intersection classifies topological relations between two DL segments into 68 topological relation classes (*TR-classes*). Among the 68 TR-classes, 34 classes (Table 1) are TR-classes without body-body intersections ($A° \cap B° = \phi$), whereas the other half (Table 2) has body-body intersections ($A° \cap B° = \neg\phi$).

Each TR-class is given a name, based on the name primitives *split* (*sp*), *diverge* (*dv*), *precede* (*pr*), *divergedBy* (*dvB*), *cross/touch* (*ct*), *mergedBy* (*mgB*), *follow* (*fl*), *merge* (*mg*), and *meet* (*mt*) that are assigned to the nine types of intersections (Eqn. 2).

$$
\begin{pmatrix}
split\ (sp) & diverge\ (dv) & preceed\ (pr) \\
divergedBy\ (dvB) & cross/touch\ (ct) & mergedBy\ (mgB) \\
follow\ (fl) & merge\ (mg) & meet\ (mt)
\end{pmatrix}
\tag{2}
$$

The names of each TR-class are then described as a set of these name primitives, like *split-cross/touch-meet*, thereby indicating the intersections that establish each TR-class. The sequence in such a compound name, however, does not reflect the sequence of the intersection types that one might observe by following one segment form head to tail, but follows a standardized naming convention (row-order across Equation 2, i.e., *sp-dv-pr-dvB-ct-mgB-fl-mg-mt*). To more concisely refer to TR-classes, we also give each TR-class a numeric label. Tables 1 and 2 show the mappings from names to numeric labels.

Properties of the hbt-matrices reflect certain algebraic properties of the corresponding relations. For example, if an hbt-matrix N can be obtained by transposing another hbt-matrix M along its main diagonal (i.e., $N = M^T$), then the two corresponding TR-classes form a pair of converse relations. Likewise, if $M = M^T$, then the corresponding relation is symmetric. In total, there are twenty symmetric TR-classes, and each of the remaining 48 TR-classes has a converse TR-class within these 48 TR-classes, forming 24 pairs of converse TR-classes.

The TR-class whose matrix has non-empty entries along the main diagonal, but empty entries otherwise (i.e., #44: *split-cross/touch-meet*), deserves special attention, as it includes the situation in which two DL segments completely coincide, which would correspond to the equality of two DL segments and imply this class's transitive property (Fig. 2a). This coincidence is, however, not the only configuration that matches the hbt-matrix specification, because other topological configurations than equal (Fig. 2b) are also covered by the same hbt-matrix of non-empty values for the three intersections of the head-head, body-body, and tail-tail pairs. As a consequence, this TR-class is not a transitive relation (Fig. 2c). This issue is revisited in Section 6.
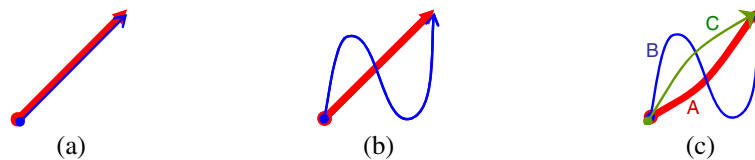
Fig. 2. Two configurations (a) and (b) covered by TR-class #44, and (c) an example that this TR-class is not transitive

Table 1. The 34 TR-classes without body-body intersections (#1 through #34) with examples of geometric prototypes

|	symmetric TR-classes	converse pairs of asymmetric TR-classes		
0	#1 *disjoint* $\begin{pmatrix} \phi & \phi & \phi \\ \phi & \phi & \phi \\ \phi & \phi & \phi \end{pmatrix}$			
1	#2 *split* $\begin{pmatrix} \neg\phi & \phi & \phi \\ \phi & \phi & \phi \\ \phi & \phi & \phi \end{pmatrix}$ #3 *meet* $\begin{pmatrix} \phi & \phi & \phi \\ \phi & \phi & \phi \\ \phi & \phi & \neg\phi \end{pmatrix}$	#4 *precede* $\begin{pmatrix} \phi & \phi & \neg\phi \\ \phi & \phi & \phi \\ \phi & \phi & \phi \end{pmatrix}$ ↑↓ #5 *follow* $\begin{pmatrix} \phi & \phi & \phi \\ \phi & \phi & \phi \\ \neg\phi & \phi & \phi \end{pmatrix}$	#6 *diverge* $\begin{pmatrix} \phi & \neg\phi & \phi \\ \phi & \phi & \phi \\ \phi & \phi & \phi \end{pmatrix}$ ↑↓ #7 *divergedBy* $\begin{pmatrix} \phi & \phi & \phi \\ \neg\phi & \phi & \phi \\ \phi & \phi & \phi \end{pmatrix}$	#8 *mergedBy* $\begin{pmatrix} \phi & \phi & \phi \\ \phi & \phi & \neg\phi \\ \phi & \phi & \phi \end{pmatrix}$ ↑↓ #9 *merge* $\begin{pmatrix} \phi & \phi & \phi \\ \phi & \phi & \phi \\ \phi & \neg\phi & \phi \end{pmatrix}$
2	#10 *split-meet* $\begin{pmatrix} \neg\phi & \phi & \phi \\ \phi & \phi & \phi \\ \phi & \phi & \neg\phi \end{pmatrix}$ #11 *precede-follow* $\begin{pmatrix} \phi & \phi & \neg\phi \\ \phi & \phi & \phi \\ \neg\phi & \phi & \phi \end{pmatrix}$ #12 *diverge-divergedBy* $\begin{pmatrix} \phi & \neg\phi & \phi \\ \neg\phi & \phi & \phi \\ \phi & \phi & \phi \end{pmatrix}$ #13 *mergedBy-merge* $\begin{pmatrix} \phi & \phi & \phi \\ \phi & \phi & \neg\phi \\ \phi & \neg\phi & \phi \end{pmatrix}$	#14 *diverge-merge* $\begin{pmatrix} \phi & \neg\phi & \phi \\ \phi & \phi & \phi \\ \phi & \neg\phi & \phi \end{pmatrix}$ ↑↓ #15 *divergedBy-mergedBy* $\begin{pmatrix} \phi & \phi & \phi \\ \neg\phi & \phi & \neg\phi \\ \phi & \phi & \phi \end{pmatrix}$ #16 *diverge-mergedBy* $\begin{pmatrix} \phi & \neg\phi & \phi \\ \phi & \phi & \neg\phi \\ \phi & \phi & \phi \end{pmatrix}$ ↑↓ #17 *divergedBy-merge* $\begin{pmatrix} \phi & \phi & \phi \\ \neg\phi & \phi & \phi \\ \phi & \neg\phi & \phi \end{pmatrix}$	#18 *split-mergedBy* $\begin{pmatrix} \neg\phi & \phi & \phi \\ \phi & \phi & \neg\phi \\ \phi & \phi & \phi \end{pmatrix}$ ↑↓ #19 *split-merge* $\begin{pmatrix} \neg\phi & \phi & \phi \\ \phi & \phi & \phi \\ \phi & \neg\phi & \phi \end{pmatrix}$ #20 *divergedBy-meet* $\begin{pmatrix} \phi & \phi & \phi \\ \neg\phi & \phi & \phi \\ \phi & \phi & \neg\phi \end{pmatrix}$ ↑↓ #21 *diverge-meet* $\begin{pmatrix} \phi & \neg\phi & \phi \\ \phi & \phi & \phi \\ \phi & \phi & \neg\phi \end{pmatrix}$	#22 *diverge-follow* $\begin{pmatrix} \phi & \neg\phi & \phi \\ \phi & \phi & \phi \\ \neg\phi & \phi & \phi \end{pmatrix}$ ↑↓ #23 *precede-divergedBy* $\begin{pmatrix} \phi & \phi & \neg\phi \\ \neg\phi & \phi & \phi \\ \phi & \phi & \phi \end{pmatrix}$ #24 *precede-merge* $\begin{pmatrix} \phi & \phi & \neg\phi \\ \phi & \phi & \phi \\ \phi & \neg\phi & \phi \end{pmatrix}$ ↑↓ #25 *mergedBy-follow* $\begin{pmatrix} \phi & \phi & \phi \\ \phi & \phi & \neg\phi \\ \neg\phi & \phi & \phi \end{pmatrix}$
3	#26 *split-mergedBy-merge* $\begin{pmatrix} \neg\phi & \phi & \phi \\ \phi & \phi & \neg\phi \\ \phi & \neg\phi & \phi \end{pmatrix}$ #27 *diverge-divergedBy-meet* $\begin{pmatrix} \phi & \neg\phi & \phi \\ \neg\phi & \phi & \phi \\ \phi & \phi & \neg\phi \end{pmatrix}$	#28 *precede-divergedBy-merge* $\begin{pmatrix} \phi & \phi & \neg\phi \\ \neg\phi & \phi & \phi \\ \phi & \neg\phi & \phi \end{pmatrix}$ ↑↓ #29 *diverge-mergedBy-follow* $\begin{pmatrix} \phi & \neg\phi & \phi \\ \phi & \phi & \neg\phi \\ \neg\phi & \phi & \phi \end{pmatrix}$	#30 *diverge-divergedBy-mergedBy* $\begin{pmatrix} \phi & \neg\phi & \phi \\ \neg\phi & \phi & \neg\phi \\ \phi & \phi & \phi \end{pmatrix}$ ↑↓ #31 *diverge-divergedBy-merge* $\begin{pmatrix} \phi & \neg\phi & \phi \\ \neg\phi & \phi & \phi \\ \phi & \neg\phi & \phi \end{pmatrix}$	#32 *divergedBy-mergedBy-merge* $\begin{pmatrix} \phi & \phi & \phi \\ \neg\phi & \phi & \neg\phi \\ \phi & \neg\phi & \phi \end{pmatrix}$ ↑↓ #33 *diverge-mergedBy-merge* $\begin{pmatrix} \phi & \neg\phi & \phi \\ \phi & \phi & \neg\phi \\ \phi & \neg\phi & \phi \end{pmatrix}$
4	#34 *diverge-divergedBy-mergedBy-merge* $\begin{pmatrix} \phi & \neg\phi & \phi \\ \neg\phi & \phi & \neg\phi \\ \phi & \neg\phi & \phi \end{pmatrix}$			

(left axis label: number of intersections)

Table 2. The 34 TR-classes with body-body intersections (#35 through #68) with examples of geometric prototypes

	symmetric TR-classes	converse pairs of asymmetric TR-classes		
1	#35 cross/touch $\begin{pmatrix} \phi & \phi & \phi \\ \phi & \neg\phi & \phi \\ \phi & \phi & \phi \end{pmatrix}$			
2	#36 split-cross/touch $\begin{pmatrix} \neg\phi & \phi & \phi \\ \phi & \neg\phi & \phi \\ \phi & \phi & \phi \end{pmatrix}$	#38 precede-cross/touch $\begin{pmatrix} \phi & \phi & \neg\phi \\ \phi & \neg\phi & \phi \\ \phi & \phi & \phi \end{pmatrix}$ ↑↓	#40 diverge-cross/touch $\begin{pmatrix} \phi & \neg\phi & \phi \\ \phi & \neg\phi & \phi \\ \phi & \phi & \phi \end{pmatrix}$ ↑↓	#42 cross/touch-mergedBy $\begin{pmatrix} \phi & \phi & \phi \\ \phi & \neg\phi & \neg\phi \\ \phi & \phi & \phi \end{pmatrix}$ ↑↓
	#37 cross/touch-meet $\begin{pmatrix} \phi & \phi & \phi \\ \phi & \neg\phi & \phi \\ \phi & \phi & \neg\phi \end{pmatrix}$	#39 cross/touch-follow $\begin{pmatrix} \phi & \phi & \phi \\ \phi & \neg\phi & \phi \\ \neg\phi & \phi & \phi \end{pmatrix}$	#41 divergedBy-cross/touch $\begin{pmatrix} \phi & \phi & \phi \\ \neg\phi & \neg\phi & \phi \\ \phi & \phi & \phi \end{pmatrix}$	#43 cross/touch-merge $\begin{pmatrix} \phi & \phi & \phi \\ \phi & \neg\phi & \phi \\ \phi & \neg\phi & \phi \end{pmatrix}$
3	#44 split-cross/touch-meet $\begin{pmatrix} \neg\phi & \phi & \phi \\ \phi & \neg\phi & \phi \\ \phi & \phi & \neg\phi \end{pmatrix}$	#48 diverge-cross/touch-merge $\begin{pmatrix} \phi & \neg\phi & \phi \\ \phi & \neg\phi & \phi \\ \phi & \neg\phi & \phi \end{pmatrix}$ ↑↓	#52 split-cross/touch-mergedBy $\begin{pmatrix} \neg\phi & \phi & \phi \\ \phi & \neg\phi & \neg\phi \\ \phi & \phi & \phi \end{pmatrix}$ ↑↓	#56 diverge-cross/touch-follow $\begin{pmatrix} \phi & \neg\phi & \phi \\ \phi & \neg\phi & \phi \\ \neg\phi & \phi & \phi \end{pmatrix}$ ↑↓
	#45 precede-cross/touch-follow $\begin{pmatrix} \phi & \phi & \neg\phi \\ \phi & \neg\phi & \phi \\ \neg\phi & \phi & \phi \end{pmatrix}$	#49 divergedBy-cross/touch-mergedBy $\begin{pmatrix} \phi & \phi & \phi \\ \neg\phi & \neg\phi & \neg\phi \\ \phi & \phi & \phi \end{pmatrix}$	#53 split-cross/touch-merge $\begin{pmatrix} \neg\phi & \phi & \phi \\ \phi & \neg\phi & \phi \\ \phi & \neg\phi & \phi \end{pmatrix}$	#57 precede-divergedBy-cross/touch $\begin{pmatrix} \phi & \phi & \neg\phi \\ \neg\phi & \neg\phi & \phi \\ \phi & \phi & \phi \end{pmatrix}$
	#46 diverge-divergedBy-cross/touch $\begin{pmatrix} \phi & \neg\phi & \phi \\ \neg\phi & \neg\phi & \phi \\ \phi & \phi & \phi \end{pmatrix}$	#50 diverge-cross/touch-mergedBy $\begin{pmatrix} \phi & \neg\phi & \phi \\ \phi & \neg\phi & \neg\phi \\ \phi & \phi & \phi \end{pmatrix}$ ↑↓	#54 divergedBy-cross/touch-meet $\begin{pmatrix} \phi & \phi & \phi \\ \neg\phi & \neg\phi & \phi \\ \phi & \phi & \neg\phi \end{pmatrix}$ ↑↓	#58 precede-cross/touch-merge $\begin{pmatrix} \phi & \phi & \neg\phi \\ \phi & \neg\phi & \phi \\ \phi & \neg\phi & \phi \end{pmatrix}$
	#47 cross/touch-mergedBy-merge $\begin{pmatrix} \phi & \phi & \phi \\ \phi & \neg\phi & \neg\phi \\ \phi & \neg\phi & \phi \end{pmatrix}$	#51 divergedBy-cross/touch-merge $\begin{pmatrix} \phi & \phi & \phi \\ \neg\phi & \neg\phi & \phi \\ \phi & \neg\phi & \phi \end{pmatrix}$	#55 diverge-cross/touch-meet $\begin{pmatrix} \phi & \neg\phi & \phi \\ \phi & \neg\phi & \phi \\ \phi & \phi & \neg\phi \end{pmatrix}$	#59 cross/touch-mergedBy-follow $\begin{pmatrix} \phi & \phi & \phi \\ \phi & \neg\phi & \neg\phi \\ \neg\phi & \phi & \phi \end{pmatrix}$
4	#60 split-cross/touch-mergedBy-merge $\begin{pmatrix} \neg\phi & \phi & \phi \\ \phi & \neg\phi & \neg\phi \\ \phi & \neg\phi & \phi \end{pmatrix}$	#62 precede-divergedBy-cross/touch-merge $\begin{pmatrix} \phi & \phi & \neg\phi \\ \neg\phi & \neg\phi & \phi \\ \phi & \neg\phi & \phi \end{pmatrix}$ ↑↓	#64 diverge-divergedBy-cross/touch-mergedBy $\begin{pmatrix} \phi & \neg\phi & \phi \\ \neg\phi & \neg\phi & \neg\phi \\ \phi & \phi & \phi \end{pmatrix}$ ↑↓	#66 divergedBy-cross/touch-mergedBy-merge $\begin{pmatrix} \phi & \phi & \phi \\ \neg\phi & \neg\phi & \neg\phi \\ \phi & \neg\phi & \phi \end{pmatrix}$ ↑↓
	#61 diverge-divergedBy-cross/touch-meet $\begin{pmatrix} \phi & \neg\phi & \phi \\ \neg\phi & \neg\phi & \phi \\ \phi & \phi & \neg\phi \end{pmatrix}$	#63 diverge-cross/touch-mergedBy-follow $\begin{pmatrix} \phi & \neg\phi & \phi \\ \phi & \neg\phi & \neg\phi \\ \neg\phi & \phi & \phi \end{pmatrix}$	#65 diverge-divergedBy-cross/touch-merge $\begin{pmatrix} \phi & \neg\phi & \phi \\ \neg\phi & \neg\phi & \phi \\ \phi & \neg\phi & \phi \end{pmatrix}$	#67 diverge-cross/touch-mergedBy-merge $\begin{pmatrix} \phi & \neg\phi & \phi \\ \phi & \neg\phi & \neg\phi \\ \phi & \neg\phi & \phi \end{pmatrix}$
5	#68 diverge-divergedBy-cross/touch-mergedBy-merge $\begin{pmatrix} \phi & \neg\phi & \phi \\ \neg\phi & \neg\phi & \neg\phi \\ \phi & \neg\phi & \phi \end{pmatrix}$			

number of intersections

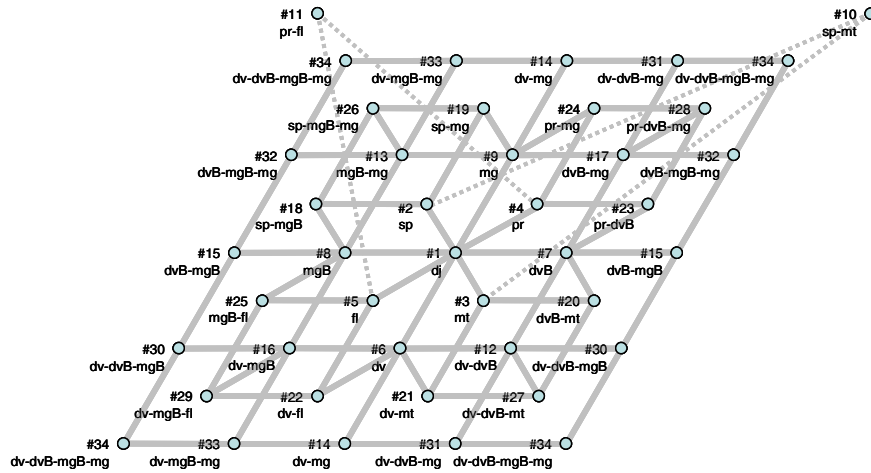## 4   Conceptual Neighborhoods of the 68 TR-Classes

If a continuous transformation can be performed between two spatial relations without having to go through a third relation, then this establishes a *direct transition*. These two relations have been called *conceptual neighbors* (Freksa 1992a). For example, the two TR-classes *split* (#2) and *split-mergedBy* (#18) are conceptual neighbors, because moving the head of the first DL segment from the other segment's exterior to its body is a direct transition. On the other hand, TR-classes *spilt* (#2) and *meet* (#3) are not neighbors, because disconnecting the head-tail intersection of *split* and establishing the head-head intersection of *meet* would need to go through either *split-meet* (#10) or *disjoint* (#1). We focus here on the equivalents of type-A neighbors for 1-dimensional intervals (Freksa 1992a), that is, those pairs of relations that can be transformed into each other by changing in their hbt-matrices one intersection from empty to non-empty, or vice-versa, but not several of them simultaneously. Equivalents of Type-B neighbors would require an entire DL segment to move—establishing, for instance, a link between *disjoint* (#1) and *diverge-cross/touch-mergedBy* (#50)—whereas the equivalents of Type-C neighbors are such that both boundary points of a DL segment would need to be moved—for example, turning *disjoint* (#1) and *diverge-merge* (#14) into neighbors.

The conceptual neighborhood graph of the 68 TR-classes is derived computationally from the relations' hbt-matrices, counting the number of differences in corresponding matrix cells with regards to empty/non-empty values (Egenhofer and Al-Taha 1992). Pairs of TR-classes with no differences in corresponding matrix cells would mean that the two TR-classes are identical, whereas pairs of TR-classes with a single difference across their hbt-matrices reflect an atomic change, dissolving either an intersection of two boundary elements, or an intersection between a boundary element and a body, or an intersection between two bodies. Pairs of TR-classes with a difference of 1 are called *conceptual 1-neighbors*.

The 1-neighbors among TR-classes #1 through #34 (as well among TR-classes #35 through #68) have the following countable properties: One TR-class has eight 1-neighbors; four TR-classes have six 1-neighbors and another four TR-classes have five 1-neighbors; eleven TR-classes have four 1-neighbors; twelve TR-classes have three 1-neighbors; and two TR-classes have two 1-neigbors. Across the two groups of TR-classes, each TR-class has exactly one 1-neighbor such that #n and #($n+34$) are neighbors ($1 \leq n \leq 34$). This means each TR-class has, in addition to the 1-neighbors within its group, another 1-neighbor that extends to the other group, increasing the neighbor count by one.

In the conceptual neighborhood graph, each TR-class has a node and each 1-neighbor of two TR-classes maps onto an edge that links the TR-classes' two nodes; therefore, the number of 1-neighbors of a TR-class corresponds to the node's degree within the neighborhood graph. These properties bring forth a conceptual neighborhood graph of one layer for TR-classes #1 through #34 (Fig. 3), and another one for TR-classes #35 through #68.
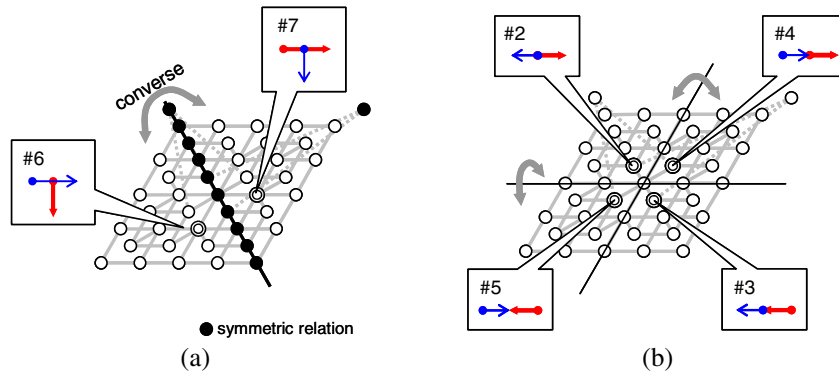
Fig. 3. The flattened conceptual neighborhood graph of the TR-classes #1 through #34. It displays more than 34 nodes in order to highlight some of the regularities of the neighborhoods by repeating the nodes in the front and back row as well as in the left and right column

The graph highlights the special status of the TR-classes *split-meet* (#10) and *precede-follow* (#11) as the only TR-classes with two conceptual neighbors among their 34 companions without body-body intersections. A visual inspection might suggest that this graph misses some links (e.g., along the diagonal from #5 to #16 or from #29 to #34), but their hbt-matrices confirm that such pairs cannot qualify as 1-neighbors, because any transition among them would require moving through another TR-class (e.g., through #6 or #8 to get from #5 to #16).

This graph of 1-neighbors also keeps its role as a reference framework when other kinds of neighbors would be considered (e.g., 2-neighbors whose matrix difference would be 2). In such a case, shortcuts along this graph would be introduced (e.g., another eight links among the eight TR-classes #2 thought #9 with exactly one non-empty intersection). Subsequently, only the graph derived from the 1-neighbors is analyzed. The conceptual neighborhood graphs of TR-classes #1 through #34, as well as TR-classes #35 through #68, have the following characteristics:

- TR-classes with fewer intersections are located closer to the center. This property is, however, one of choice, because different elements than TR-class #1 could have been selected as the central reference point.
- TR-classes located along the diagonal from top-left to bottom-right are symmetric (Fig. 4a).
- Pairs of TR-classes that are located symmetrically across the diagonal from top-left to bottom-right are converse, that is, the same matrices are obtained by transposing the matrices along their main diagonals (Fig. 4a).
- The conceptual neighborhood graph can be decomposed into four subgraphs with a horizontal and vertical mirror axis such that the same matrices are obtained by reversing the direction of one DL segment (Fig. 4b).

Fig. 4. Characteristics of the flattened conceptual neighborhood graph of TR-classes #1 through #34: (a) symmetric and converse TR-classes and (b) the four subgraphs that are obtained by reversing the direction of a DL segment when mirroring the TR-class along the graph's horizontal or vertical axis, as highlighted by TR-classes #2-#5

Gluing the flattened graph's front and back rows, and then the leftmost and rightmost columns, yields a non-redundant configuration in which the graph extends over the surface of a torus (Fig. 5b). TR-classes #10 and #11, which placed irregularly above the flattened graph (Fig. 3), are now outside the torus (Fig. 5b), highlighting through their irregular locations again the two nodes' unique properties of degree 2.
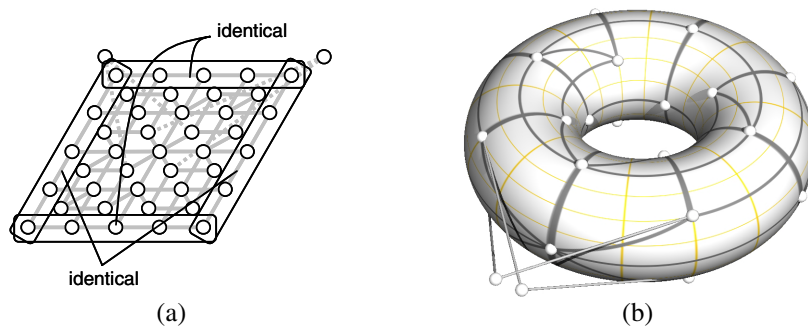
Fig. 5. The transition from (a) the flattened conceptual neighborhood graph of TR-classes #1 through #34 with repeated columns and rows to (b) a graph displayed on the surface of a torus, which is obtained by gluing together the repeated rows and columns along the fringes of the flattened graph.

The integrated conceptual neighborhood graph of TR-classes #1 through #68 has a two-layered structure, where each layer contains a homeomorphic conceptual neighborhood graph of #1 through #34 or #35 through #68, and each node in one of these layers is linked to one node in another layer, thereby representing the neighbor relation between #n and #(n+34). Consequently, the conceptual neighborhood graph of the TR-classes #1 through #68 is represented in a 3-dimensional space where nodes are aligned on two parallel planes (Fig. 6a). When the flattened structure is connected

through the redundant nodes at its fringes, the graph forms a shape that extends over the surfaces of two tori, one inside the other, with links across the two tori to establish the neighborhoods of #n and #(n+34) with $1 \leq n \leq 34$ (Fig. 6b).

(a)   (b)
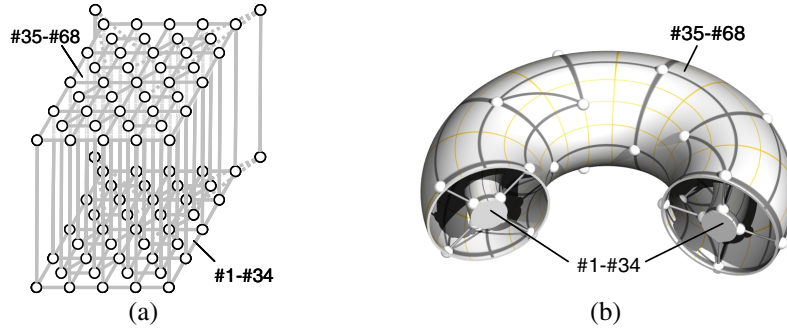
Fig. 6. Two structures of the conceptual neighborhood graph of TR-classes #1 through #68, where nodes are aligned on (a) two parallel planes and (b) the surfaces of two nested tori

5 Inferences About the 68 TR-Classes

The 68 DL segment relations allow us to capture the topological relations between these segments in a simple, consistent, and qualitative way that is suitable for processing queries about their relations recorded in a database. Queries may, however also refer to relations that have not been recorded explicitly so that it may be necessary to deduce result candidates from a logical combination of available information about several relations. In support of such queries involving implied relations, this section develops the *composition table* of the 68 TR-classes. Given three DL segments, A, B, and C, whose TR-classes are denoted by R_{AB}, R_{BC}, and R_{AC}, the composition of R_{AB} and R_{BC}, denoted by R_{AB} ; R_{BC}, is the set of all possible TR-classes between A and C. The actual value of R_{AC} is always included in R_{AB} ; R_{BC}.

5.1 Constraints on the Hbt-Matrix for Composed TR-Classes

Let the TR-classes R_{AB}, R_{BC}, and R_{AC} correspond to the respective hbt-matrices M_{AB}, M_{BC}, and M_{AC} (Eqn. 3).

$$M_{AB} = \begin{pmatrix} I_{AB}^{tt} & I_{AB}^{tb} & I_{AB}^{th} \\ I_{AB}^{bt} & I_{AB}^{bb} & I_{AB}^{bh} \\ I_{AB}^{ht} & I_{AB}^{hb} & I_{AB}^{hh} \end{pmatrix} \quad M_{BC} = \begin{pmatrix} I_{BC}^{tt} & I_{BC}^{tb} & I_{BC}^{th} \\ I_{BC}^{bt} & I_{BC}^{bb} & I_{BC}^{bh} \\ I_{BC}^{ht} & I_{BC}^{hb} & I_{BC}^{hh} \end{pmatrix} \quad M_{AC} = \begin{pmatrix} I_{AC}^{tt} & I_{AC}^{tb} & I_{AC}^{th} \\ I_{AC}^{bt} & I_{AC}^{bb} & I_{AC}^{bh} \\ I_{AC}^{ht} & I_{AC}^{hb} & I_{AC}^{hh} \end{pmatrix} \quad (3)$$

Symbols p_A, p_B, p_C denote arbitrary parts of A, B, and C (i.e., either tail or body or head). If B's tail intersects with both p_A and p_C, then p_A and p_C must intersect, since B's tail is a point on which both p_A and p_C are partly or wholly located. Similarly, if B's head intersects with both p_A and p_C, then p_A and p_C must intersect as well. These geometric constraints lead to the constraint on M_{AC} that p_A and p_C intersect if B's tail or head intersects with both p_A and p_C (Eqn. 4).

For $p_A, p_C \in \{t, b, h\}$

$$\left(I_{AB}^{p_A t} = \neg\phi \ \land \ I_{BC}^{tp_C} = \neg\phi\right) \ \lor \ \left(I_{AB}^{p_A h} = \neg\phi \ \land \ I_{BC}^{hp_C} = \neg\phi\right) \ \rightarrow \ I_{AC}^{p_A p_C} = \neg\phi \qquad (4)$$

The intersection between A's tail and p_B, if it exists, is totally included in p_B, since A's tail is a point. Thus, if p_B intersects with A's tail, but not p_C, A's tail and p_C do not intersect. Similarly,

- A's head and p_C do not intersect if p_B intersects with A's head but not p_C,
- C's tail and p_A do not intersect if p_B intersects with C's tail but not p_A, and
- C's head and p_A do not intersect if p_B intersects with C's head but not p_A.

These four conditions imply another constraint on M_{AC} (Eqn. 5).

$$\text{For } p_A, p_B, p_C \in \{t, b, h\}$$

$$I_{AB}^{tp_B} = \neg\phi \ \land \ I_{BC}^{p_B p_C} = \phi \ \rightarrow \ I_{AC}^{tp_C} = \phi$$

$$I_{AB}^{hp_B} = \neg\phi \ \land \ I_{BC}^{p_B p_C} = \phi \ \rightarrow \ I_{AC}^{hp_C} = \phi$$

$$I_{AB}^{p_A p_B} = \phi \ \land \ I_{BC}^{p_B t} = \neg\phi \ \rightarrow \ I_{AC}^{p_A t} = \phi \qquad (5)$$

$$I_{AB}^{p_A p_B} = \phi \ \land \ I_{BC}^{p_B h} = \neg\phi \ \rightarrow \ I_{AC}^{p_A h} = \phi$$

Among the 68 configurations of the hbt-intersection (Tables 1 and 2), the configurations that satisfy the two constraints (Eqs. 4 and 5) are the candidates for M_{AC} and, therefore, the TR-classes that correspond to these candidates of M_{AC} configurations are the compositions of TR-classes R_{AB} and R_{BC}.

5.2 Composition Table for TR-Classes of DL Segment Relations

The compositions of the TR-classes were determined from the hbt-matrices (Tables 1 and 2) and the constraints on the hbt-matrix of the composition (Eqs. 4 and 5). The resulting composition table for the TR-classes between DL segments contains 68×68 = 4,624 composition elements, of which Table 3 shows a small subset for TR-classes #7, #9, #10, #19, and #44.

The validity of the composition table is demonstrated, although not proved formally, by the following observations:

- Any composition is connected in the conceptual neighborhood graph.
- Any composition satisfies the following constraint:

$$\forall X \quad R_{AA} = sp\text{-}ct\text{-}mt \in R_{AX}; R_{XA} \qquad (6)$$

Eqs. 4 and 5 do not contain the constraint on the non-existence of a body-body intersection. Accordingly, if a composition contains a TR-class without a body-body intersection (say R^-), then the composition also contains the TR-class that adds a body-body intersection to R^-. This means that if a TR-class in the lower layer is in a composition, then the vertical neighbor of this TR-class (located in the upper layer) is also in that composition (Table 3). For example, the composition *split-merge*; *split-meet*, contains *split* and *split*'s vertical neighbor, that is, *split-cross/touch*.

Table 3. A 5×5 subset of the composition table of the 68 TR-classes between DL segments
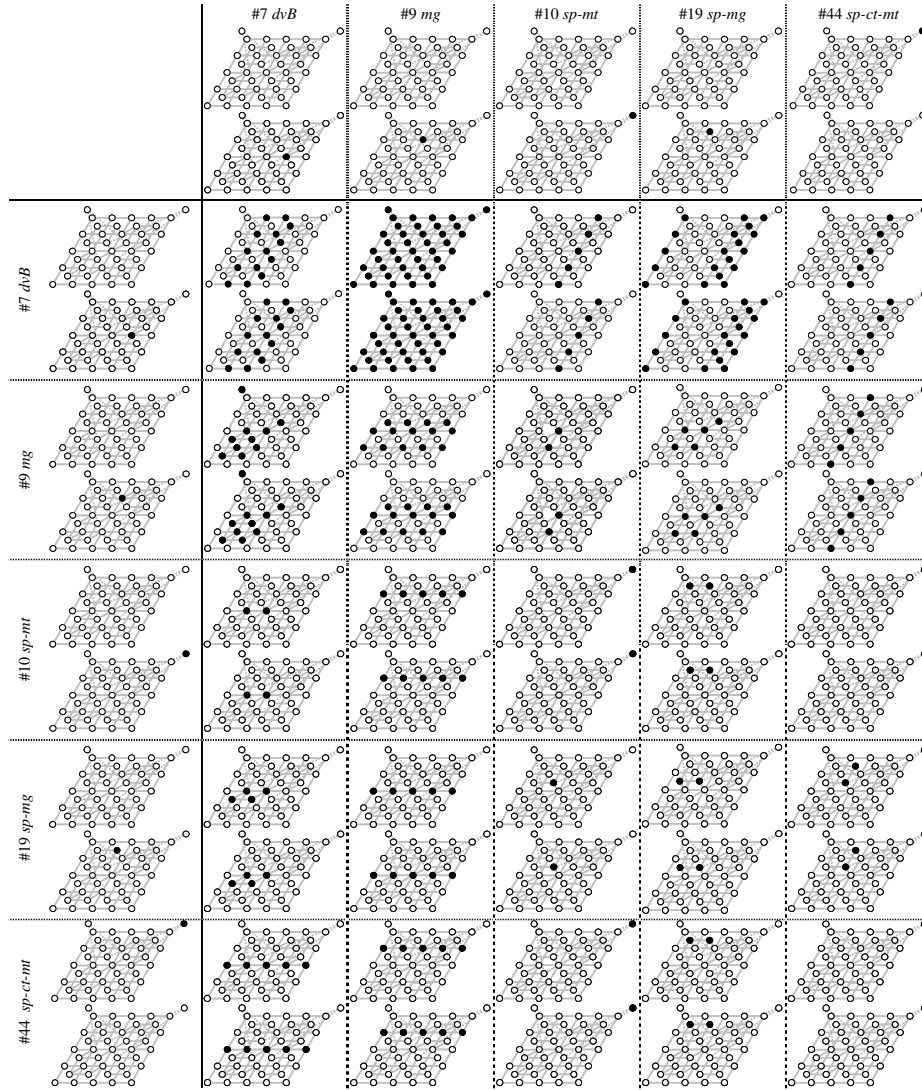
5.3 A Reasoning Example

To demonstrate the use of the composition table, consider a snow mountain with four skiing trails, *A*, *B*, *C*, and *D* (Fig. 7). A skier went down on *B* and found that:

- Trail *A* shares the same start point with *B*, takes a different course, and eventually ends at a *B*'s midpoint.
- Trail *C* starts at a *B*'s midpoint and does not intersect with B after that point.

The inference scenario is to determine symbolically (i.e., in a non-graphical way) what are the possible relations between trails *A* and *C*.
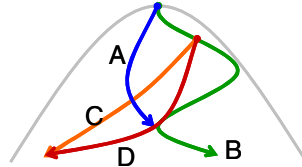
Fig. 7. A snow mountain with four skiing trails

The TR-class between *A* and *B* is *split-merge* (#19) and the TR-class between *B* and *C* is *divergedBy* (#7). According to Table 2, the composition of *split-merge* and *divergedBy* is *disjoint* (#1), *follow* (#5), *mergedBy* (#8), *mergedBy-follow* (#25), *cross/touch* (#35), *cross/touch-follow* (#39), *cross/touch-mergedBy* (#42), and *cross/touch-mergedBy-follow* (#59). Thus, these eight TR-classes are the candidates of the relation between *A* and *C*.

When the skier went down on trail *D*, she found that:

- Trail *A* ends at *D*'s midpoint and does not intersect before that point.
- Trail *C* shares the same start point with trail *D*, takes a different course, and eventually ends at the same destination with trail *D*.

This additional information further influences the inference about the possible relations between trails *A* and *C*. The TR-class between *A* and *D* is *merge* (#9) and the TR-class between *D* and *C* is *split-meet* (#10). According to Table 2, the composition of *merge* and *split-merge* is *disjoint* (#1), *diverge* (#6), *cross/touch* (#35), and *diverge-cross/touch* (#40). These four TR-classes are also the candidates of the relation between *A* and *C*. By integrating this result with the previous result, the possible TR-classes between *A* and *C* are narrowed down to *disjoint* and *cross/touch*. This indicates that the richer knowledge about the network reduces the ambiguity of its unrecorded relations.

6   The HBT⁺-Intersection

Although the hbt-intersection features nine types of intersections, it resembles the 4-intersection (Egenhofer and Franzosa 1991) more than the 9-intersection (Egenhofer and Herring 1991), because both the hbt-intersection and the 4-interesection assess the intersections between the interiors and boundaries, but not the intersections with exteriors. Since the 4-intersection cannot distinguish some topological relations between line segments that the 9-intersection can distinguish (Egenhofer 1994), it could be expected that the hbt-intersection cannot distinguish some topological relations between DL segments as well. The observation about TR-class *split-cross/touch-meet* (#44) already gave evidence for an hbt-intersection that captures at least two significantly different topological relations (Figs. 2a-b). By adding to the hbt-intersection the intersections with the DL-segments' exteriors, however, the
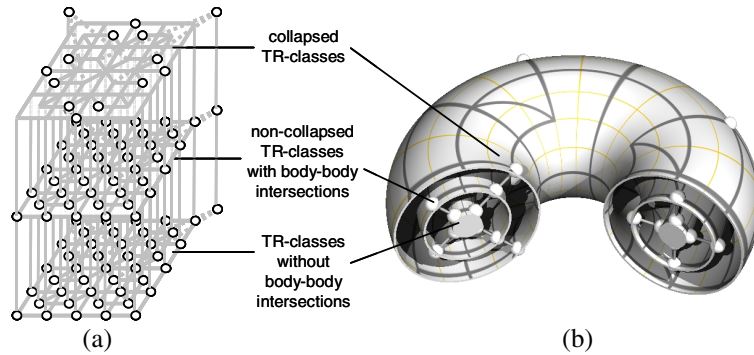
difference between these two configurations could be captured: Fig. 2a's bodies have empty intersections with the opposite DL-segment's exteriors, whereas Fig. 2b's bodies have non-empty intersections with the opposite DL-segments' exteriors. The extension by considering the exteriors of DL segments in addition to their heads, bodies, and tails requires a total of 16 types of intersections, which are represented by the *hbt$^+$-matrix*, a 4×4 matrix whose top-left 3×3 submatrix is identical to the configuration's hbt-matrix.

Among the $2^{16} = 65,536$ configurations with empty and non-empty values for the hbt$^+$-matrix, only 80 configurations have geometric interpretations. This number includes the 68 configurations obtained with the hbt-intersection plus another twelve configurations, each of which is a more constrained version of an hbt-intersection. These twelve configurations are shown in Table 4. The TR-classes that are captured by the hbt$^+$-matrix include a specification of the equivalence relations for DL segments as a refinement of TR-class #44, constraining the two bodies to coincide, and none of the two bodies to extend through the other DL-segment's exterior.

The addition of these twelve TR-classes also has an impact on the conceptual neighborhood graph. Since twelve TR-classes in the hbt-intersection are subdivided into 24 TR-classes in the hbt$^+$-intersection, the layer containing these twelve TR-classes (i.e., the upper layer in Fig. 6a) is split into two layers: one for the twelve collapsed TR-classes and another for 34 non-collapsed TR-classes with body-body intersections. Consequently, the conceptual neighborhood graph's structural framework consists of three parallel planes stacked on top of each other in the flattened version (Fig. 8a), or three tori nested transitively into each other (Fig. 8b).

Table 4. Collapsed topological relations and non-collapsed topological relations that can be distinguish by the hbt$^+$-intersection, but not by the hbt-intersection

Fig. 8. Structures of the conceptual neighborhood graph of the 80 TR-classes obtained by the hbt$^+$-intersection, where nodes are aligned on (a) three parallel planes or (b) the surfaces of three tori nested transitively in each other.

7   Conclusions

This paper classified the topological relations between two directed line segments into 80 classes, 68 of them were identified by the head-body-tail intersection, whereas intersections with the line segments' exteriors were needed to distinguish the remaining 12 cases. The 80 relations' conceptual neighborhood graph revealed a structure of three parallel planes or three nested tori. For the first time, such a comprehensive account of a conceptual neighborhood graph involving DL segment relations in a 2-dimensional space has been determined.

Future work about directed line relations will address the expressive power of the matrices' empty and non-empty intersections. If the hbt-matrix and hbt$^+$-matrix continue to record the existence/non-existence of the intersections, then the corresponding intersection models cannot distinguish some critical topological relations (Fig. 9). The development of more detailed model of the topological relations between DL segments will contribute to an improvement of the reasoning power about directed line segments.

$$\rightarrow \begin{pmatrix} \phi & \phi & \phi & \neg\phi \\ \phi & \neg\phi & \phi & \neg\phi \\ \phi & \phi & \phi & \neg\phi \\ \neg\phi & \neg\phi & \neg\phi & \neg\phi \end{pmatrix}$$
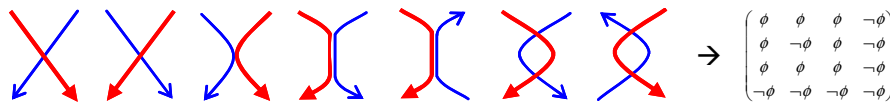
Fig. 9. Sets of DL segments, whose topological relations cannot be distinguished by the hbt-intersections or hbt$^+$-intersections

Acknowledgments

References

Alexandroff, P. (1961) *Elementary Concepts of Topology*. Dover: Mineola, NY.

Allen, J. (1983) Maintaining Knowledge About Temporal Intervals. *Communications of the ACM*. 26(11):832-843.

Clementini, E. and di Felice, P. (1998) Topological Invariants for Lines. *IEEE Transactions on Knowledge and Data Engineering*. 10(1):38-54.

Clementini, E., di Felice, P., and van Oosterom, P. (1993) A Small Set of Formal Topological Relationships Suitable for End-User Interaction. in: Abel, D. and Ooi, B.-C. (eds.) *Advances in Spatial Databases, Third International Symposium, SSD'93*, Singapore, Lecture Notes in Computer Science, 692, 277-295.

Egenhofer, M. (1994) Definitions of Line-Line Relations for Geographic Databases. *IEEE Data Engineering Bulletin*. 16(3):40-45.

Egenhofer, M. (1997) Query Processing in Spatial-Query-by-Sketch. *Journal of Visual Languages and Computing*. 8(4):403-424.

Egenhofer, M. (2005) Spherical Topological Relations. *Journal on Data Semantics* III.25-49.

Egenhofer, M. and Al-Taha, K. (1992) Reasoning About Gradual Changes of Topological Relationships. in: Frank, A., Campari, I. and Formentini, U. (eds.) *Theories and Methods of Spatio-temporal Reasoning in Geographic Space*, Pisa, Italy, Lecture Notes in Computer Science, 639, 196-219.

Egenhofer, M. and Franzosa, R. (1991) Point-Set Topological Spatial Relations. *International Journal of Geographical Information Systems*. 5(2):161-174.

Egenhofer, M. and R. Franzosa, R. (1995) On the Equivalence of Topological Relations. *International Journal of Geographical Information Systems*. 9(2): 133-152, 1995.

Egenhofer, M. and Herring, J. (1991) Categorizing Binary Topological Relationships between Regions, Lines and Points in Geographic Databases. in: Egenhofer, M., Herring, J., Smith, T. and Park, K. (eds.) *A Framework for the Definitions of Topological Relationships and an Algebraic Approach to Spatial Reasoning within This Framework*, NCGIA Technical Reports 91-7. National Center for Geographic Information and Analysis: Santa Barbara, CA.

Egenhofer, M. and Mark, D. (1995) Modeling Conceptual Neighborhoods of Topological Line-Region Relations. *International Journal of Geographical Information Systems*. 9(5):555-565.

Egenhofer, M., Sharma, J. and Mark D. (1993) A Critical Comparison of the 4-Intersection and the 9-Intersection Models for Spatial Relations: Formal Analysis. in: McMaster, R. and Armstrong, M. (eds.) *Autocarto 11*, Minneapolis, MD, 63-71.

Erwig, M. and Schneider, M. (1999) Developments in Spatio-Temporal Query Languages. in: *10th International Workshop on Database & Expert Systems Application*, Florence, Italy, IEEE Computer Society, 441-449.

Freksa, C. (1992a) Temporal Reasoning Based on Semi-Intervals. *Artificial Intelligence*. 54:199-227.

Freksa, C. (1992b) Using Orientation Information for Qualitative Spatial Reasoning. in: Frank, A., Campari, I. and Formentini, U. (eds.) *The International Conference GIS—From Space to Territory: Theories and Methods of Spatio-Temporal Reasoning in Geographic Space*, New York, NY, Lecture Notes in Computer Science, 639, 162-178.

Goyal, R. and Egenhofer, M. (2000) Consistent Queries over Cardinal Directions across Different Levels of Detail. in: Tjoa, A.M., Wagner, R., and Al-Zobaidie, A. (eds.), *11th International Workshop on Database and Expert Systems Applications*, Greenwich, U.K. 876-880.

Hadzilacos, T. and Tryfona, N. (1992) Model for Expressing Topological Integrity Constraints in Geographic Databases. in: Frank, A., Campari, I. and Formentini, U. (eds.) *The International Conference GIS—From Space to Territory: Theories and Methods of Spatio-Temporal Reasoning in Geographic Space*, New York, NY, Lecture Notes in Computer Science, 639, 252-268.

Herring, J. (1991) The Mathematical Modeling of Spatial and Non-Spatial Information in Geographic Information Systems. in: Mark, D. and Frank A. (eds.) *Cognitive and Linguistic Aspects of Geographic Space*, Kluwer: Dordrecht, Netherlands, 313-350.

Hoel, E. and Samet, H. (1991) Efficient Processing of Spatial Queries in Line Segment Databases. in: Gunther, O. and Schek, H.-J. (eds.) *Advances in Spatial Databases—2nd Symposium, SSD'91*, New York, NY, Lecture Notes in Computer Science, 525, 237-256.

Hornsby, K., Egenhofer, M. and Hayes, P. (1999) Modeling Cyclic Change. in: Chen, P., Embley, D., Kouloumdjian, J., Liddle, S. and Roddick, J. (eds.) *Advances in Conceptual Modeling*, Paris, France, Lecture Notes in Computer Science, 1227, 98-109.

Krieg-Brückner, B. and Shi, H. (2005) Orientation Calculi + Route Graphs: Towards Semantic Representations of Route Descriptions. *Dagstuhl Seminar on Spatial Cognition: Specialization and Integration*, http://www.dagstuhl.de/files/Materials/05/05491/ 05491. KriegBruecknerBernd.Slides.pdf

Kurata, Y. and Egenhofer, M. (2005a) Semantics of Simple Arrow Diagrams. in: Barkowsky, T., Freksa, C., Hegarty, M. and Lowe, R. (eds.) *AAAI Spring Symposium on Reasoning with Mental and External Diagram: Computational Modeling and Spatial Assistance*, Stanford, CA, 101-104.

Kurata, Y. and Egenhofer, M. (2005b) Structure and Semantics of Arrow Diagrams. in: Cohn, A. and Mark, D. (eds.) *COSIT '05*, Ellicottville, NY, Lecture Notes in Computer Science, 3693, 232-250.

Kurata, Y. and Egenhofer, M. (2006) Topological Relations of Arrow Symbols in Complex Diagrams. in: D. Barker-Plummer, R. Cox, and N. Swoboda (eds.), *Diagrams 2006: Fourth International Conference on the Theory and Application of Diagrams*, Stanford, CA, Lecture Notes in Artificial Intelligence, 4045, 112-126.

Mark, D. and Egenhofer, M. (1994) Modeling Spatial Relations between Lines and Regions: Combining Formal Methods and Human Subjects Testing, *Cartography and Geographic Information Systems*. 21(4):195-212.

Moratz, R., Renz, J. and Wolter, D. (2000) Qualitative Spatial Reasoning About Line Segments. in: Horn, W. (ed.) *14th European Conference on Artificial Intelligence*, Berlin, Germany, 234-238.

Nedas, K., Egenhofer, M. and Wilmsen, D. (in press) Metric Details of Topological Line-Line Relations. *International Journal of Geographical Information Science*.

Papadias, D., Theodoridis, Y., Sellis, T., and Egenhofer, M. (1995) Topological Relations in the World of Minimum Bounding Rectangles: A Study with R-Trees. In: Carey, M. and Schneider, D. (eds.) *SIGMOD RECORD* 24 (2): 92-103.

Pullar, D. and Egenhofer, M. (1988) Towards Formal Definitions of Topological Relations among Spatial Objects. *Third International Symposium on Spatial Data Handling*, Sydney, Australia, 225-241.

Renz, J. (2001) A Spatial Odyssey of the Interval Algebra: 1. Directed Intervals. in: Nebel, B. (ed.) *International Joint Conference on Artificial Intelligence 2001*, Seattle, WA, 51-56.

Reis, R., Egenhofer, M., and Mattos, J. (2005) Grafos de Vinzihanças Conceptuais para Relações Topológicas entre Linhas em R^2. *Fourth National Conference for Cartography and Geodesy*, Lisbon, Portugal, http://www.igeo.pt/Igeo/portugues/Novidades_eventos/ eventos/Lisboa/ivcncg_reis.pdf.

Schlieder, C. (1995) Reasoning About Ordering. in: Frank, A. and Kuhn, W. (eds.) *COSIT '95*, Lecture Notes in Computer Science, 988, 341-349.

Shariff, A., Egenhofer, M. and Mark, D. (1998) Natural-Language Spatial Relations between Linear and Areal Objects: The Topology and Metric of English-Language Terms. *International Journal of Geographical Information Science*. 12(3):215-246.